Available online at www.sciencedirect.com

ScienceDirect

Nuclear Physics B 906 (2016) 147–167

NUCLEAR PHYSICS B

www.elsevier.com/locate/nuclphysb

Six loop analytical calculation of the field anomalous dimension and the critical exponent η in $O(n)$-symmetric φ^4 model

D.V. Batkovich [a], K.G. Chetyrkin [b], M.V. Kompaniets [a,*]

[a] *St. Petersburg State University, 7/9 Universitetskaya nab., St. Petersburg, 199034, Russia*

[b] *Institut für Theoretische Teilchenphysik, Karlsruher Institut für Technologie (KIT), D-76128 Karlsruhe, Germany*

Received 3 February 2016; accepted 4 March 2016

Available online 9 March 2016

Editor: Hubert Saleur

Abstract

We report on a completely analytical calculation of the field anomalous dimension γ_φ and the critical exponent η for the $O(n)$-symmetric φ^4 model at the record six loop level. We successfully compare our result for γ_φ with $n = 1$ with the predictions based on the method of the Borel resummation combined with a conformal mapping (Kazakov et al., 1979 [40]). Predictions for seven loop contribution to the field anomalous dimensions are given.

1. Introduction

Since Kenneth Wilson, who was first to apply ϵ-expansion and renormalization group method to calculate critical exponents in φ^4 model, this model became one of the most popular testing grounds for a wide range of methods of diagram calculations and resummation. The first two terms of the ϵ-expansion were calculated by Wilson in [1], ϵ^3 terms and ϵ^4 for critical exponent

* Corresponding author.

E-mail addresses: batya239@gmail.com (D.V. Batkovich), konstantin.chetyrkin@kit.edu (K.G. Chetyrkin), m.kompaniets@spbu.ru (M.V. Kompaniets).

http://dx.doi.org/10.1016/j.nuclphysb.2016.03.009

η were calculated in [2]. The latter work was the last where calculations using Wilson renormalization group approach were performed for this model. All subsequent calculations were performed using quantum field renormalization group approach, which effectively reduces the problem of evaluation of critical exponents to the one of finding the corresponding beta-function (or the anomalous dimension).

This approach combined with modern computational techniques allows one to calculate high order corrections with significantly less effort than in the original Wilson's formalism. Using this approach ϵ^4 terms for other exponents were found in [3]. The field anomalous dimension γ_φ and the critical exponent η were calculated with 5-loop accuracy in [4], the 5-loop β-function was first published in [5,6]. Later some (numerically insignificant) inaccuracies were found in this calculation and results for index η and β-function were corrected [7]. Recently, a completely independent check of the analytic results [4–7] was successfully performed in [8] with the use of purely numerical methods.

In this work we describe the results of a completely analytical calculation of γ_φ and η at six loop level in the $O(n)$-symmetric φ^4 model.

2. Setup and notations

The (renormalized) Lagrangian of the φ^4-model in the Euclidean space of $d = 4 - 2\varepsilon$ dimensions reads

$$\mathcal{L}(\varphi) = \frac{1}{2} m^2 Z_1 \varphi^2 + \frac{1}{2} Z_2 (\partial\varphi)^2 + \frac{16\pi^2}{4!} Z_4\, g\, \mu^{2\varepsilon}\, \varphi^4, \tag{1}$$

where RCs (Renormalization Constants) Z_i are expressed in terms of renormalization constants of the field $\varphi_0 = \varphi Z_\varphi$, mass $m_0^2 = m^2 Z_{m^2}$ and coupling constant $g_0 = g\mu^{2\epsilon} Z_g$ in the standard way:

$$Z_1 = Z_{m^2} Z_\varphi^2, \qquad Z_2 = Z_\varphi^2, \qquad Z_4 = Z_g Z_\varphi^4. \tag{2}$$

In the MS-scheme [9] which we employ throughout the paper the UV counterterms do not depend on μ and may depend only *polynomially* on any other dimensionfull parameter of a theory [10]. As a result the RCs Z_i do depend on the regulating parameter ε and renormalized coupling constant g *only* and can be written as:

$$Z_i = 1 + \sum_{k=1} \frac{Z_{i,k}(g)}{\varepsilon^k}. \tag{3}$$

Given the RC $Z_\varphi(g)$, the corresponding anomalous dimension of the scalar field we are interested in is defined as follows

$$\gamma_\varphi(g) = \mu \frac{\partial \log Z_\varphi(g)}{\partial \mu}\Big|_{g_0,\varphi_0} = \beta(g) \frac{\partial \log Z_\varphi}{\partial g} = -2g \frac{\partial Z_{\varphi,1}(g)}{\partial g} = -g \frac{\partial Z_{2,1}(g)}{\partial g}. \tag{4}$$

The RC Z_2 and Z_{m^2} are related with UV divergences of the two point one particle irreducible Green function $\Gamma_2(p, m_0^2, g_0)$, which is connected with two point Green function (propagator) $D(p, m_0^2, g_0)$ by Dyson equation $D^{-1}(p, m_0^2, g_0) = p^2 + m_0^2 - \Gamma_2(p, m_0^2, g_0)$. Thus for renormalized two point Green function $D^R(p, m^2, g, \mu)$ we got

$$D^R(p, m^2, g, \mu) = \frac{1}{Z_\varphi^2} D(p, m^2 Z_{m^2}, g\mu^{2\varepsilon} Z_g)$$
$$= \frac{1}{Z_\varphi^2 (p^2 + m^2 Z_{m^2} - \Gamma_2(p, m^2 Z_{m^2}, g\mu^{2\varepsilon} Z_g))}$$
$$= \frac{1}{p^2 Z_2 + m^2 Z_1 - Z_\varphi^2 \Gamma_2(p, m^2 Z_{m^2}, g\mu^{2\varepsilon} Z_g)}. \tag{5}$$

Last term in (5) can be rewritten with use of the Bogoliubov–Parasiuk R-operation [11,12] in the following way $Z_\varphi^2 \Gamma_2(p, m^2 Z_{m^2}, g\mu^{2\varepsilon} Z_g) = K R' \Gamma_2(p, m^2, g\mu^{2\varepsilon})$. So RCs Z_1 and Z_2 can be conveniently extracted from Γ_2:

$$Z_2 = 1 + \partial_{p^2} K R' \Gamma_2(p, m^2, g, \mu), \quad Z_1 = 1 + \partial_{m^2} K R' \Gamma_2(p, m^2, g, \mu), \tag{6}$$

where R' is the incomplete R-operation (which subtracts all proper UV subdivergences from a given Feynman amplitude but does not touch its UV divergence as a whole) and K stands for the operator extracting the singular part of an ε expansion:

$$K \sum_i C_i \varepsilon^i = \sum_{i<0} C_i \varepsilon^i.$$

Renormalization constants Z_i, $i = 1, 2, 3$, are known up to 5th-loop order [4–7]. The aim of this paper is to extend the results of [4] by one more order, that is, to evaluate analytically the sixth loop contribution to the anomalous dimension γ_φ and the corresponding critical exponent η.

3. RG calculations in MS-scheme: general framework

At present there are basically two different ways to perform the analytical RG calculations at the multi-loop level. Both approaches make use of the method of Infrared Rearrangement (IRR) [13,14] in order to make integral more suitable for analytical calculations by setting zero (possibly after a proper Taylor expansion) initial masses and external momenta and introducing artificial ones. Both eventually employ the traditional integration by parts method to compute the resulting Feynman integrals.

The first one [15–17] amounts to adding an artificial mass or an external momentum to a properly chosen propagator of a given Feynman diagram before the (formal) Taylor expansion in all masses (except for the artificial one) and external momenta is made. The artificial external momentum has to be introduced in such a way that all spurious infrared divergences are softened away and the obtained Feynman integral is calculable. In practice the condition of absence of the infrared divergences leads to unnecessary complications and, in some cases, even prevents from reduction to the simplest integrals. The problem was solved by elaborating a special technique of subtraction of IR divergences — the $\widetilde{R}$-operation [18–20] which we will discuss later.

In the second approach the infrared rearrangement is archived by inserting one and the same auxiliary mass to *all* propagators [21–23]. After this no IR divergences can ever appear. Next, a proper expansion in all external momenta and particle masses (except the auxiliary one) is to be performed. The resulting integrals are completely massive purely vacuum integrals (tadpoles), i.e. Feynman integrals without external momenta. Note that the expansion in external momenta and masses (except for the auxiliary one!) in both approaches is an unavoidable step if the (UV) RC we are looking for is related to a non-logarithmically divergent Feynman amplitude. It effectively reduces the quadratically (or even higher) UV divergent amplitude to the logarithmic

one which opens the way to apply IRR to the latter. This is always possible within dimensional regularization and minimal subtractions schemes (see, e.g. [24]).

Starting from $L = 3$, L-massive tadpoles are getting significantly more complicated for analytical evaluation than the L-loop vacuum integrals with all but one massless propagators. As a result, the most advanced RG calculations are being performed nowadays at the five loop level within the first, "massless" approach (see, e.g. [25,26]).

Let us discuss now the current limits of the massless way of doing RG calculations for the example of a logarithmically divergent L-loop Feynman integral $\langle\gamma\rangle$. We assume that all its UV subdivergences are already known (the corresponding Feynman (sub)-integrals will all have loop number strictly less than L). Thus, our aim is to compute the UV counterterm (we assume that the original FI $\langle\gamma\rangle$ is free from IR singularities)

$$Z_\gamma = -K\,R'\,\langle\gamma\rangle.$$

The first two steps are trivial:

(i) all (external momenta) and masses are set to zero;

and

(ii) the integrand of FI $\langle\gamma\rangle$ is modified by introducing a "softening factor"

$$\frac{p^2}{(p-q)^2}, \tag{7}$$

where the momentum p is the one flowing through an (arbitrary) internal line ℓ (in principle, one could equivalently use a combination $p^2/(m_{aux}^2 + p^2)$, with m_{aux} being an auxiliary (non-zero) mass).

The modified FI $\langle\gamma^q\rangle$ is naturally represented as a convolution:

$$\langle\gamma^q\rangle = \int \frac{\mathrm{d}p}{(2\pi)^D}\,\langle\gamma'\rangle(p)\,\frac{p^2}{(p-q)^2}, \tag{8}$$

where the (L − 1)-loop p-integral[1]

$$\langle\gamma'\rangle(p) = C_{\gamma'}(\varepsilon)\,\frac{1}{(p^2)^{2+(L-1)\varepsilon}}$$

is obtained by cutting the "softened" line ℓ in the original diagram, that is $\gamma' = \gamma \setminus \ell$. Now, if by a proper choice of ℓ the FI $\langle\gamma^q\rangle$ is made free from any IR divergences (such a choice is not always possible, see an example below) then

$$Z_\gamma = -K\,R'\,\langle\gamma^q\rangle = -K\,\langle\gamma^q\rangle + \ldots. \tag{9}$$

Here dots stand for subtractions of UV *sub*divergences; the corresponding FI's all have loop number strictly less than L and, consequently, are known according to our initial assumption. Thus, the evaluation of Z_γ amounts to the calculation of the following expression:

[1] That is a massless integral, depending on only *one* external momenta FI.

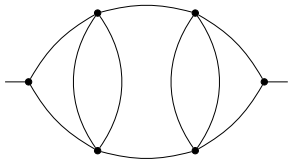

Fig. 1. No IR safe IRR (with one softened line) is possible for this graph.

$$C_{\gamma'}(\varepsilon)\int\frac{\mathrm{d}p}{(2\pi)^D}\frac{1}{(p^2)^{2+(L-1)\varepsilon}}\cdot\frac{p^2}{(p-q)^2}=C_{\gamma'}(\varepsilon)\,(q^2)^{-L\varepsilon}\;\;G(1+(L-1)\,\varepsilon,1)$$
$$=C_{\gamma'}(\varepsilon)\,(q^2)^{-L\,\varepsilon}\;\;\frac{1}{L\,\varepsilon}\cdot(1+\mathcal{O}(\varepsilon)),\qquad(10)$$

or, equivalently, the function $C_{\gamma'}(\varepsilon)$ with accuracy $\mathcal{O}(\varepsilon^0)$. In the r.h.s. of (10) we employ a convenient shortcut notation for a basic one loop p-integral [4]:

$$\int\frac{d\,p}{(2\pi)^d}\frac{1}{(p^{2\alpha})(q-p)^{2\beta}}$$
$$=\frac{(q^2)^{2-\varepsilon-\alpha-\beta}}{16\pi^2}\left(G(\alpha,\beta)=(4\pi)^{\varepsilon}\,\frac{\Gamma(\alpha+\beta-2+\varepsilon)}{\Gamma(\alpha)\Gamma(\beta)}\,\frac{\Gamma(2-\alpha-\varepsilon)\,\Gamma(2-\beta-\varepsilon)}{\Gamma(4-\alpha-\beta-2\varepsilon)}\right).\qquad(11)$$

Unfortunately, the condition of IR finiteness of the modified FI $\langle\gamma^q\rangle$ is rather restrictive, in many cases it prevents from a convenient choice of the cut-line ℓ leading to a simpler for calculation (L − 1)-loop p-integral or even from the very possibility of application of IRR to a diagram (see Fig. 1). The restriction can be lifted completely with the use of R^*-operation which includes IR subtractions in addition to usual UV ones:

$$R^*=R\cdot\widetilde{R}.\qquad(12)$$

Here $\widetilde{R}$ stands for the IR R-operation which recursively subtracts all IR singularities from a given (Euclidean!) FI. Thus, for the case of an arbitrary chosen line ℓ eq. (9) assumes the form

$$Z_\gamma=-K\,R'\,\widetilde{R}\,\langle\gamma^q\rangle=-K\,R'\,\widetilde{R}'\,\langle\gamma^q\rangle=-K\,\langle\gamma^q\rangle+\ldots.\qquad(13)$$

Eq. (13) requires a few comments.

First, the $\widetilde{R}'$ operation is defined as $\widetilde{R}$ *without* the last IR subtraction corresponding to IR divergence of the FI $\langle\gamma^q\rangle$ as a whole. The transition to $\widetilde{R}'$ in the middle of (13) is perfectly legal as the presence of the modified propagator in the FI $\langle\gamma^q\rangle$ ensures the superficial IR convergence of the latter.

Second, the application of both R' and $\widetilde{R}'$ in (13) is a purely algebraic procedure as all UV and IR counterterms to be computed can be algebraically expressed[2] in terms of (proper) UV counterterms of $\langle\gamma\rangle$ (which are known according to our initial assumption). As a result, we again arrive at a conclusion, that even for a generic choice of the cut-line ℓ the evaluation of Z_γ requires knowledge of the pole and finite parts of the (L-1)-loop p-integral $\langle\gamma^q\rangle$ (as well as some p-integrals with less number of loops).

Third, given a vertex with more than three incident fields, it can be easily transformed (cut) into two vertices joined by a new line with the corresponding propagator equal identically 1

[2] We will not discuss in any detail the internal mechanics of $\widetilde{R}'$-operation (see in this connection [18,27,28]).

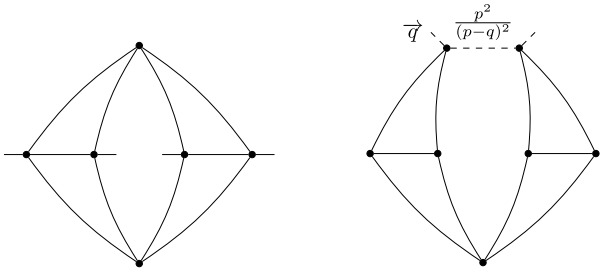

Fig. 2. IRR performed using vertex cut, dashed line represents corresponding softening factor.

(see Fig. 2). This new line can also be used as a cut-one. We will see in the next section that in many cases cutting a vertex leads to especially simple (in fact, factorizable) p-integrals.

Recently the state of the art of analytical calculation of p-integrals has established itself at the four loop level (for more details see [29]), which means that 5-loop RG calculations are now feasible, while 6-loop calculations are still not possible in the general case. We will see in the next section why for a particular simple model of the scalar φ^4 theory the 5-loop barrier was taken more than thirty years ago and why these days even 6-loop level has got accessible.

To summarize this section: given an L-loop completely massless vacuum diagram Γ with zero (in four-dimensions) superficial index of the (UV) divergence of the corresponding formal FI $\langle\Gamma\rangle$ the use of R^* operation reduces the calculation of the UV counterterm Z_Γ to evaluation of only one $(\mathrm{L}-1)$-loop p-integral $\langle\Gamma^p\rangle(p)$ obtained by cutting an arbitrary line ℓ from Γ (not counting p-integrals with loop number less than L which should be computed for removing UV and IR *sub*divergences from $\langle\Gamma^q\rangle$). The final result for the UV counterterm

$$K\,R'\,\widetilde{R}'\langle\gamma^q\rangle$$

does not depend on the choice of the line ℓ which provides us with a strong check of the correctness of the calculations.

4. Calculation of TV-Reducible diagrams

The main simplifying feature of the φ^4 model comes from the fact that its only interaction vertex is composed of *four* scalar fields. As a result the variety of different "topologies" of FIs to be computed is strongly reduced with respect to, say, the φ^3 model. This is well illustrated by the fact that the first analytical four-loop RG calculation in the latter model have been performed very recently [30] (the four-loop RG-functions for the φ^4 model are known since 1979 [16]).

Different cut-lines lead generically not only to different $(\mathrm{L}-1)$-loop p-integrals: a wisely chosen cut line could in many cases result in especially simple p-integral. This happens if the original vacuum graph Γ is TVR (*Two-Vertex-Reducible*). By definition, a 1PI vacuum graph Γ belongs to a class of TVR ones if it is possible to cut one of its lines or vertexes in such a way that the resulting graph $\Gamma\setminus\ell$ becomes One-Vertex-Reducible (OVR), that is, the corresponding FI $F_{\Gamma\setminus\ell}(p)$ can be presented as a product of two p-integrals each with non-zero number of loops.

Thus, for a TVR graph the calculation of FI the $F_{\Gamma\setminus\ell}(p)$ amounts to computing two p-integrals F_{γ_1} and F_{γ_2} with loop numbers $L_1>0$ and $L_2>0$, $L_1+L_2=L-1$ respectively. This also means that any UV counterterm for every 6-loop FI $\langle\Gamma\rangle$ (not necessarily logarithmically divergent one) with Γ being TVR is analytically calculable provided one knows the ε expansions of four-loop master p-integrals with ε accuracy by one order more than the one necessary for 5-loop

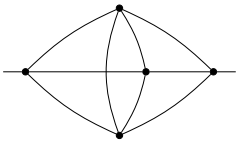

Fig. 3. The only TVI diagram contributing to the field self-energy at five loop.

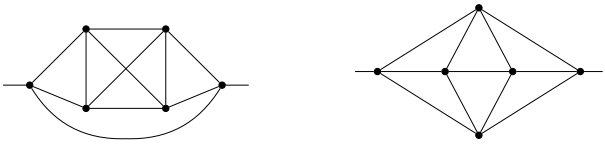

Fig. 4. (a) and (b): TVI diagrams contributing to the field self-energy at six loop level.

calculations[3] (and available from [31]). Fortunately, this missing power of ε (and many more) have been all found in [32] for the whole collection of 4-loop p-masters and confirmed in [33].

In fact, TVR graphs abound in the φ^4 model which is the underlying reason of the very possibility of the early 4 and 5-loop RG calculations as well as our current ability to perform the same calculations at the six loop level. Indeed, at three and four loops all diagrams contributing to the AD γ_2 happen to be TV-Reducible. At five loops all except for *one* (see Fig. 3) diagrams are also TV-Reducible.

At six loop level the situation is as follows: among 50 diagrams all are TV-Reducible except for two. To compute 48 TVR-diagrams we have used a (python) toolbox for calculation of UV countertems [28] which allows to automate all operations on Feynman diagrams, like infrared rearrangement, R^* operation as well as IBP reduction (we have employed the reduction rules generated by LiteRed [34]). The diagram-wise results are listed in Table A.2 of Appendix A. The table includes also the results for TV-Irreducible diagrams whose treatment will be discussed in the next section.

5. Calculation of TV-Irreducible diagrams

In six loops there are only two TV-Irreducible diagrams pictured on Fig. 4. According to the general strategy of IRR these diagrams do require the knowledge of complicated (that is non-factorizable) 5-loop p-integrals for their evaluation. Below we describe how both diagrams have been computed.

5.1. Diagram (a)

Diagram (a) (see Fig. 4(a)) has quite a special topology: it contains a line connecting both external vertexes. In addition, it is quadratically divergent. These facts combined allow for rather simple calculation of the corresponding UV counterterm. First step is trivial as one among six

[3] Actually, our current calculation has *not* (accidentally?) required this extra power of ε for four-loop master p-integrals. As a result our final result for γ_φ (see eq. (19)) does not include any irrational constants beyond those appearing in general 5-loop RG calculations (for a detailed discussion, see [31]).

loop integrations for diagram (a) can be easily done analytically (due to a line connecting both external vertexes) with the following result:

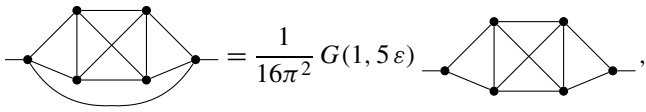

$$= \frac{1}{16\pi^2}\, G(1, 5\varepsilon)$$

,

where (see eq. (11)) $G(1, 5\varepsilon) = -\dfrac{5}{12} + \mathcal{O}(\varepsilon)$. (14)

The fact that the first factor $G(1, 5\varepsilon)$ in r.h.s. of (14) is of order $\mathcal{O}(\varepsilon^0)$ means that we need to know only pole part of the second factor. Pole part of this 5-loop p-integral is easy to compute (see Appendix B).

5.2. Diagram (b)

For the second diagram in Fig. 4 we need to calculate the derivative with respect to p. This produces two terms (the line with an arrow stands for p_μ / p^2):

$$\frac{1}{2}(\partial_p)^2 K R' \left(\right.$$

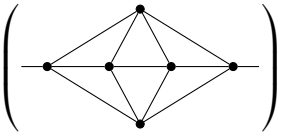

$$\left. \right) = 2K R' \left(\frac{4-d}{d} \right.$$

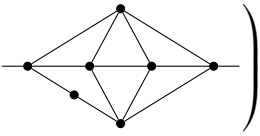

$$\left. \right) + 2K R' \left(\frac{4}{d} \right.$$

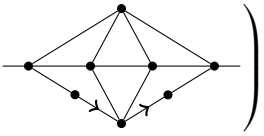

$$\left. \right). \qquad (15)$$

The first diagram in r.h.s. of (15) can be calculated in the same way as first non TVR diagram in Sec. 5.1. The second one requires additional consideration.

First of all this diagram is logarithmically divergent and primitive (i.e. contains no subdivergences), so we can perform the following IR rearrangement:

$$K R' \left(\frac{4}{d} \right.$$

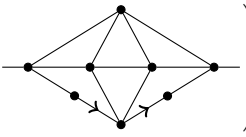

$$\left. \right) = K R' \left(\frac{4}{d} \right.$$

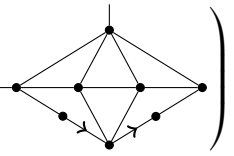

$$\left. \right). \qquad (16)$$

For the latter diagram we can integrate out one loop using (10):

$$K \left(\frac{4}{d} \right.$$

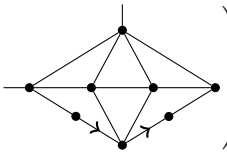

$$\left. \right) = K \left(\frac{4}{d} G(1, 1+5\varepsilon) \right.$$

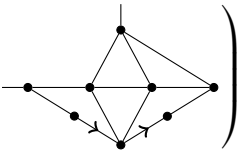

$$\left. \right). \qquad (17)$$

We need the value of the diagram in r.h.s. of (17) up to a constant term only as the corresponding factor there is of order $\mathcal{O}(\varepsilon^{-1})$. Because of the fact that the diagram is finite (no divergences at

all) we need to calculate only the leading (constant) term in its expansion in ε. This can be done using transition to the corresponding dual graph:

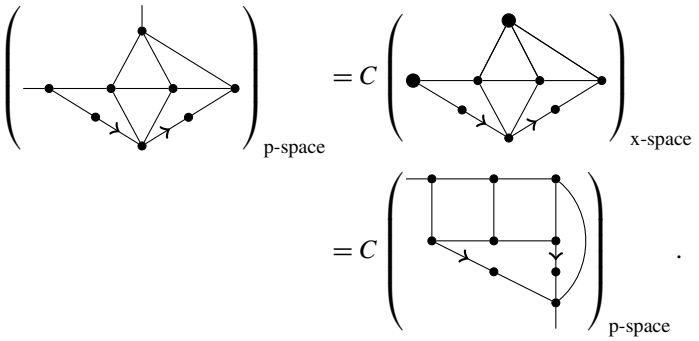

(18)

It should be noted that the x-space propagators (second and third diagrams in (18)) have a non-standard ε dependence, viz. $1/(x_1 - x_2)^{2(1-\varepsilon)}$. Fortunately, as far as we are looking only for leading (constant) contribution we can consider standard propagators $1/(x_1 - x_2)^2$. Now, the diagram in r.h.s. of (18) has only 4 loops and can be calculated using the standard 4-loop IBP reduction. The fact that transition to the dual graph can lower the number of loops is another simplifying feature of the φ^4 model. Interestingly, the 5-loop TVI diagram on Fig. 3 can be also easily performed in the same way.[4]

6. Results and discussion

After adding diagram-wise results of Table A.2 and known five loop results [7] we arrive at the following expression for the anomalous dimension of field γ_φ to the six loop level:

$$\begin{aligned}
\gamma_\varphi(g) = {} & \frac{g^2(n+2)}{36} - \left[8+n\right]\frac{g^3(n+2)}{432} + \left[500 + 90\,n - 5\,n^2\right]\frac{g^4(n+2)}{5184} + \\
& + \Big[-77\,056 + 8832\,\zeta_3 - 25\,344\,\zeta_4 + (-22\,752 + 3072\,\zeta_3 - 5760\,\zeta_4)\,n + \\
& + (-296 - 288\,\zeta_3)\,n^2 + (-39 + 48\,\zeta_3)\,n^3\Big]\frac{g^5(n+2)}{186\,624} + \Big[1\,410\,544 + \\
& + 1\,190\,400\,\zeta_6 + 297\,472\,\zeta_3 - 833\,536\,\zeta_5 - 95\,232\,\zeta_3^2 + 619\,776\,\zeta_4 + \\
& + \Big(549\,104 + 352\,000\,\zeta_6 + 69\,888\,\zeta_3 - 293\,632\,\zeta_5 - 28\,160\,\zeta_3^2 + 215\,808\,\zeta_4\Big)\,n + \\
& + \Big(30\,184 + 12\,800\,\zeta_6 + 14\,976\,\zeta_3 - 23\,680\,\zeta_5 - 1024\,\zeta_3^2 + 15\,744\,\zeta_4\Big)\,n^2 + \\
& + (-794 + 96\,\zeta_4)\,n^3 + (-29 - 16\,\zeta_3 + 48\,\zeta_4)\,n^4\Big]\frac{g^6(n+2)}{746\,496}.
\end{aligned} \tag{19}$$

Substituting g_* calculated in 5 loop approximation (see e.g. [36]) into the anomalous dimension $\gamma_2 = 2\,\gamma_\varphi$ we obtain the critical exponent η up to $\mathcal{O}(\varepsilon^7)$:

[4] Originally the diagram was analytically computed in [35] with a series of ad hoc non-obvious tricks.

$$
\begin{aligned}
\eta(\varepsilon) = {} & \frac{(2\epsilon)^2}{2}\frac{(n+2)}{(n+8)^2} + \left[272 + 56\,n - n^2\right]\frac{(2\epsilon)^3}{8}\frac{(n+2)}{(n+8)^4} + \\
& + \Big[46\,144 - 67\,584\,\zeta_3 + (17\,920 - 23\,808\,\zeta_3)\;n + \\
& + (1124 - 1920\,\zeta_3)\;n^2 - 230\,n^3 - 5\,n^4\Big]\frac{(2\epsilon)^4}{32}\frac{(n+2)}{(n+8)^6} + \\
& + \Big[5\,655\,552 + 60\,948\,480\,\zeta_5 - 21\,921\,792\,\zeta_3 - 12\,976\,128\,\zeta_4 + \\
& + (2\,912\,768 + 33\,259\,520\,\zeta_5 - 11\,530\,240\,\zeta_3 - 7\,815\,168\,\zeta_4)\;n + \\
& + (262\,528 + 6\,113\,280\,\zeta_5 - 1\,244\,160\,\zeta_3 - 1\,714\,176\,\zeta_4)\;n^2 + \\
& + (-121\,472 + 445\,440\,\zeta_5 + 137\,984\,\zeta_3 - 163\,584\,\zeta_4)\;n^3 + \\
& + (-27\,620 + 10\,240\,\zeta_5 + 20\,800\,\zeta_3 - 5760\,\zeta_4)\;n^4 + \\
& + (-946 + 288\,\zeta_3)\;n^5 + (-13 + 16\,\zeta_3)\;n^6\Big]\frac{(2\epsilon)^5}{128}\frac{(n+2)}{(n+8)^8} + \\
& + \Big[565\,354\,496 - 60\,808\,495\,104\,\zeta_7 + 19\,134\,414\,848\,\zeta_5 + \\
& + 19\,503\,513\,600\,\zeta_6 - 5\,485\,101\,056\,\zeta_3 + 5\,036\,310\,528\,\zeta_3^2 - \\
& - 4\,208\,984\,064\,\zeta_4 + \Big(323\,108\,864 - 44\,652\,625\,920\,\zeta_7 + \\
& + 13\,118\,341\,120\,\zeta_5 + 15\,518\,924\,800\,\zeta_6 - 3\,681\,222\,656\,\zeta_3 + \\
& + 4\,007\,919\,616\,\zeta_3^2 - 3\,266\,052\,096\,\zeta_4\Big)\,n + \\
& + \Big(8\,413\,184 - 12\,662\,415\,360\,\zeta_7 + 2\,504\,949\,760\,\zeta_5 + 4\,921\,753\,600\,\zeta_6 - \\
& - 533\,012\,480\,\zeta_3 + 1\,142\,210\,560\,\zeta_3^2 - 858\,095\,616\,\zeta_4\Big)\,n^2 + \\
& + \Big(-45\,721\,600 - 1\,749\,888\,000\,\zeta_7 - 84\,449\,280\,\zeta_5 + \\
& + 797\,900\,800\,\zeta_6 + 131\,311\,616\,\zeta_3 + 144\,695\,296\,\zeta_3^2 - 67\,817\,472\,\zeta_4\Big)\,n^3 + \\
& + \Big(-17\,128\,928 - 118\,540\,800\,\zeta_7 - 71\,895\,040\,\zeta_5 + \\
& + 69\,478\,400\,\zeta_6 + 40\,585\,984\,\zeta_3 + 8\,321\,024\,\zeta_3^2 + 6\,884\,352\,\zeta_4\Big)\,n^4 + \\
& + \Big(-2\,460\,768 - 3\,161\,088\,\zeta_7 - 6\,955\,264\,\zeta_5 + \\
& + 3\,046\,400\,\zeta_6 + 2\,822\,400\,\zeta_3 + 250\,880\,\zeta_3^2 + 1\,467\,648\,\zeta_4\Big)\,n^5 + \\
& + \Big(-110\,512 - 195\,200\,\zeta_5 + 51\,200\,\zeta_6 + 36\,096\,\zeta_3 + \\
& + 8192\,\zeta_3^2 + 79\,296\,\zeta_4\Big)\,n^6 + (-2748 + 2656\,\zeta_3 + 1632\,\zeta_4)\;n^7 + \\
& + (-29 - 16\,\zeta_3 + 48\,\zeta_4)\;n^8\Big]\frac{(2\epsilon)^6}{512}\frac{(n+2)}{(n+8)^{10}}. \qquad (20)
\end{aligned}
$$

For $n = 1$ the anomalous dimension γ_φ and the exponent η assume the form

$$\gamma_\varphi = \frac{1}{12}g^2 - \frac{1}{16}g^3 + \frac{65}{192}g^4 + \left[-3709 - 1152\,\zeta_4 + 432\,\zeta_3\right]\frac{g^5}{2304} +$$
$$+ \left[\mathbf{73\,667 + 31\,536\,\zeta_4 - 4608\,\zeta_3^2 + 57\,600\,\zeta_6 - 42\,624\,\zeta_5 + 14\,160\,\zeta_3}\right]\frac{\mathbf{g^6}}{\mathbf{9216}} + \mathcal{O}(u^7)$$
$$= 0.0833g^2 - 0.0625g^3 + 0.3385g^4 - 1.9255g^5 + \mathbf{14.383}g^6 + \mathcal{O}(g^7), \tag{21}$$

$$\eta = \frac{2}{27}\varepsilon^2 + \frac{109}{729}\varepsilon^3 + \left(\frac{7217}{39\,366} - \frac{64}{243}\zeta_3\right)\varepsilon^4 +$$
$$+ \left(\frac{321\,511}{2\,125\,764} - \frac{32}{81}\zeta_4 - \frac{1316}{2187}\zeta_3 + \frac{1280}{729}\zeta_5\right)\varepsilon^5 + \left(\frac{\mathbf{3\,421\,613}}{\mathbf{38\,263\,752}} - \frac{\mathbf{3136}}{\mathbf{243}}\zeta_7 +\right.$$
$$\left. + \frac{\mathbf{73\,232}}{\mathbf{19\,683}}\zeta_5 - \frac{\mathbf{181\,462}}{\mathbf{177\,147}}\zeta_3 + \frac{\mathbf{3200}}{\mathbf{729}}\zeta_6 + \frac{\mathbf{2432}}{\mathbf{2187}}\zeta_3^2 - \frac{\mathbf{658}}{\mathbf{729}}\zeta_4\right)\varepsilon^6 + \mathcal{O}(\varepsilon^7) \tag{22}$$
$$= 0.074074\,\varepsilon^2 + 0.149520\,\varepsilon^3 - 0.133260\,\varepsilon^4 + 0.821006\,\varepsilon^5 - \mathbf{5.201449}\,\varepsilon^6 +$$
$$+ \mathcal{O}(\varepsilon^7). \tag{23}$$

We perform various consistency checks of our results. First of all, the finiteness of γ_φ as found from (4) at 6 loop ensures the correctness of high order poles in ε in the RC Z_φ. The first pole in ε (which actually contributes to γ_φ and η) cannot be checked in such a way. Fortunately, there is a self-consistency test which is sensitive to the structure of the first pole. It is based on the known results of $1/n$-expansion for critical exponent η. The expansion is currently available up to $1/n^3$ term [37,36]. The coefficients of this expansion are exact functions of ε, on the other hand coefficients of ε-expansion of critical exponent η are exact functions on n. Expanding both functions in ε and $1/n$ respectively we will obtain double expansion in ε and $1/n$ which must coincide up to given $(\varepsilon^6,\ 1/n^3)$ order. From these expansions we can derive 3 independent relations on linear combinations of the coefficients at first pole in ε of the six loop diagrams. Moreover, a relation that originates from the term of order $1/n^3$ includes all graphs from A.2. All three relations are indeed in agreement with our results (more details can be found in Appendix C).

For some selected diagrams we have also performed additional numerical checks using the sector decomposition technique (see, e.g. [38]).

In papers [39,40] the method of a resummation of the asymptotic series was proposed. This method combines an assumption about asymptotic of beta function at $g \to \infty$ and the available information about higher order asymptotic [41] via a Borel transformation with conformal mapping. It was shown that for the series where asymptotic $g \to \infty$ is known, most accurate values (after resummation of the finite part of the series) are obtained if parameter ν (additional parameter which defines the behavior of the resummed series at $g \to \infty$) is chosen in accordance with $g \to \infty$ asymptotic. Moreover, in this case the contribution of high order terms gets minimized.

For the φ^4 model the asymptotic behavior at $g \to \infty$ is not known, so authors of [39,40] used the criterion of minimization of the contribution of the high order terms as a way to determine the correct value of the parameter ν. They found that for the case of the beta-function of the φ^4 model it should lie within the range $1.7 < \nu < 2.2$, commonly the value $\nu = 2$ is taken.

Furthermore, if we perform such a resummation procedure for a given number of loops L and then expand back the series obtained after conformal mapping procedure up to the next, $(L+1)$-loop order, then this term may be considered as a prediction for the $(L+1)$-loop contribution because of the minimization of high order contributions we have discussed above. In

Table 1
Resummation result for the Fisher exponent η for different number of loops taken into account.

Loops β/γ_φ	3/4	3/5	3/6	4/4	4/5	4/6	5/5	5/6	est.
$D=2$	0.1716	0.1818	0.1827	0.2211	0.2365	0.2379	0.2263	0.2276	0.25
$D=3$	0.03201	0.03256	0.03260	0.03557	0.03624	0.03629	0.03577	0.03581	0.03601

particular, the prediction of [39,40] for the 5-loop term in the beta-function happened to be 1404.3 while the direct calculations [5–7] (published a year later) produced the value 1424.28, which is different from the prediction only by a minute 1.5%.

We apply the same procedure to γ_φ with $n=1$ (see eq. (21)). Using $\nu=3$ and performing the same steps for terms up to 5 loops we arrive at the following predictions for the 6-loop term

$$\gamma_\varphi^{P5}(g) = 0.0833g^2 - 0.0625g^3 + 0.3385g^4 - 1.9255g^5 + \mathbf{14.316g^6} + \mathcal{O}(g^7), \tag{24}$$

which is only by 0.5% smaller than calculated in the present work. If we repeat the same procedure starting from 6 loops we can make a prediction for the 7 loop contribution to the field anomalous dimension.

$$\gamma_\varphi^{P6}(g) = 0.0833g^2 - 0.0625g^3 + 0.3385g^4 - 1.9255g^5 + 14.383g^6 - \mathbf{127.29g^7} + \mathcal{O}(g^8).$$

If one performs a resummation of the $\gamma_\varphi(g)$ at $g=g_*$ (where g_* is a first positive zero of the resummed beta-function), one can obtain estimations for the Fisher exponent η for different numbers of loops taken into account in $\beta(g)$ and $\gamma_\varphi(g)$.

The column in Table 1 marked as 'est.' is an estimated value for this model ($n=1$). For two-dimensional model it corresponds to the Onsager exact solution, for three-dimensional case it corresponds to a combination of the results of the high temperature expansion (HT) and the Monte Carlo simulations (MC) made in [42]. One can see that results of resummation for the 3D model are very close to HT and MC results ($\sim 0.5\%$). For the 2D model results are also in reasonable agreement with the Onsager exact solution but still far from it (~ 5–10%). This effect may be explained by large value of the expansion parameter $\epsilon=1$. Also one can see from the table that most valuable impact on the value of the Fisher exponent is given by the value of the fixed point (i.e. beta function). This fact may serve as an additional argument to compute 6-loop beta function [43], of course, for the 3D model one may expect swing around the HT/MC value, but for the 2D model, due to significant impact of the 5-loop beta function (comparing to the 4-loop one) we still can't expect reasonable result for the Fisher exponent.

7. Conclusions

We have described a completely analytical calculation of the field anomalous dimension γ_φ and the critical exponent η for the $O(n)$-symmetric φ^4 model at the six loop level. The calculation has proved to be possible due to a combination of the method of IRR based on the heavy use of the R^*-operation and recent advances in computing master four-loop massless p-integrals as well as due to a special feature of the φ^4 theory: the overwhelming number of diagrams appearing at 4- and 5-loops happen to be Two Vertex Reducible ones.

We successfully compare our result for γ_φ with $n = 1$ with the predictions based on the method of the Borel transform followed by a conformal mapping.

Our diagram-wise results for all six loop contributions to Z_2 (together with some auxiliary information) are available (in computer-readable form) in http://www.ttp.kit.edu/Progdata/ttp15/ttp15-046/.

They are also appended to the TEX-file of the present paper.

Acknowledgements

We thank J.H. Kühn for an attentive reading of the manuscript and L.Ts. Adzhemyan, D.I. Kazakov, R.N. Lee for fruitful discussions.

This work was supported by the Deutsche Forschungsgemeinschaft through CH 1479/1-1 (K.G.Ch.). We acknowledge Saint Petersburg State University for a research grant 11.38.185. 2014 (D.V.B. and M.V.K.). We also thank Resource Center "Computer Center of SPbU" for providing computational resources.

Appendix A. Diagramwise results for 6-loop contributions to Z_2

Tables A.2 and A.3 display results for all fifty self-energy diagrams contributing to RC Z_2. For brevity we have used the so-called Nickel index (NI) which allows for a short and concise description of a given diagram [44,45].

Generally speaking Nickel index is a list of graph edges written for some canonical vertex ordering. The canonical vertex ordering ensures that two isomorphic graphs have equal Nickel indices. For example, consider Nickel index '$ee12|223|3|ee|$': vertical lines split the NI on sections, each section corresponds to the one of the vertices. Vertices are assumed to be labeled from 0 (up to 3 for this graph), each section describes graph edges connected to this vertex, i.e. vertex 0 has two external (e) edges and edges to vertices 1 and 2. Next section lists edges connected to vertex 1 (except ones that connected to the vertex 0): two edges to vertex 2 and edge to 3. Third section lists edges connected to vertex 2 (except ones connected to 0 and 1) and so on. Drawing graph in such a way we arrive at the diagram on Fig. A.5.

Construction of the NI from the graph is a bit more complicated task: one needs to take all possible graph labeling, for each labeling write a Nickel notation described above, and then choose minimal (in some sense) notation as NI. Luckily this procedure can be optimized to avoid $n!$ growth (see [45]).

Every row in A.2 describes a contribution of a diagram γ with NI NI(γ) to Z_2 as a product of three factors, namely, s_γ (a symmetry factor), $\mathtt{r}_\gamma$ (an additional structure factor for n-component $O(n)$-symmetric φ^4-model in terms of polynomials given in A.3) and, finally, the very counterterm $\partial_{p^2} K R' \gamma$.

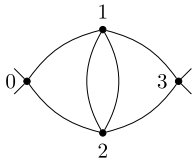

Fig. A.5. Graph that corresponds to Nickel index (NI) equal to $ee12|223|3|ee|$.

Table A.2
Values of the six loop graphs contributing to Z_2.

N	NI(γ)	s_γ	$\mathtt{r}_\gamma$	$\partial_{p^2} K R' \gamma$
1	$e112\|23\|34\|45\|55\|e\|$	1/4	$r_1\, r_{10}$	$-\frac{1}{90}\,\varepsilon^{-5}+\frac{13}{180}\,\varepsilon^{-4}-\frac{13}{45}\,\varepsilon^{-3}+\frac{133}{180}\,\varepsilon^{-2}-\frac{4}{3}\,\varepsilon^{-1}$
2	$e112\|23\|34\|55\|e55\|\|$	1/4	$r_1\, r_{13}$	$-\frac{1}{48}\,\varepsilon^{-5}+\frac{121}{1440}\,\varepsilon^{-4}-\frac{11}{64}\,\varepsilon^{-3}+\left(\frac{289}{5760}+\frac{13}{120}\,\zeta_3\right)\varepsilon^{-2}+\left(\frac{5809}{11\,520}-\frac{1}{40}\,\zeta_4-\frac{53}{240}\,\zeta_3\right)\varepsilon^{-1}$
3	$e112\|23\|34\|e5\|555\|\|$	1/6	$r_1^2\, r_3$	$-\frac{31}{2880}\,\varepsilon^{-4}+\frac{191}{2880}\,\varepsilon^{-3}-\frac{47}{256}\,\varepsilon^{-2}+\frac{1675}{4608}\,\varepsilon^{-1}$
4	$e112\|23\|44\|455\|5\|e\|$	1/8	$r_1\, r_{11}$	$-\frac{1}{40}\,\varepsilon^{-5}+\frac{7}{80}\,\varepsilon^{-4}-\frac{67}{480}\,\varepsilon^{-3}+\left(\frac{29}{960}+\frac{1}{20}\,\zeta_3\right)\varepsilon^{-2}+\left(-\frac{49}{640}+\frac{3}{40}\,\zeta_4-\frac{43}{120}\,\zeta_3\right)\varepsilon^{-1}$
5	$e112\|23\|44\|555\|e5\|\|$	1/12	$r_1^2\, r_3$	$-\frac{1}{64}\,\varepsilon^{-4}+\frac{3}{64}\,\varepsilon^{-3}-\frac{19}{3840}\,\varepsilon^{-2}+\left(\frac{707}{7680}+\frac{1}{30}\,\zeta_3\right)\varepsilon^{-1}$
6	$e112\|23\|44\|e55\|55\|\|$	1/8	$r_1\, r_9$	$-\frac{11}{240}\,\varepsilon^{-5}+\frac{41}{480}\,\varepsilon^{-4}-\frac{23}{960}\,\varepsilon^{-3}+\left(-\frac{11}{384}-\frac{1}{24}\,\zeta_3\right)\varepsilon^{-2}+\left(-\frac{187}{768}+\frac{1}{8}\,\zeta_4+\frac{1}{48}\,\zeta_3\right)\varepsilon^{-1}$
7	$e112\|23\|45\|445\|5\|e\|$	1/2	$r_1\, r_{10}$	$-\frac{7}{720}\,\varepsilon^{-5}+\frac{17}{288}\,\varepsilon^{-4}-\frac{563}{2880}\,\varepsilon^{-3}+\left(\frac{2269}{5760}-\frac{13}{60}\,\zeta_3\right)\varepsilon^{-2}+\left(-\frac{497}{3840}+\frac{1}{20}\,\zeta_4+\frac{9}{40}\,\zeta_3\right)\varepsilon^{-1}$
8	$e112\|23\|45\|e45\|55\|\|$	1/4	$r_1\, r_{11}$	$-\frac{11}{720}\,\varepsilon^{-5}+\frac{103}{1440}\,\varepsilon^{-4}-\frac{127}{960}\,\varepsilon^{-3}+\left(\frac{31}{1152}+\frac{1}{5}\,\zeta_3\right)\varepsilon^{-2}+\left(\frac{2843}{11\,520}-\frac{3}{40}\,\zeta_4-\frac{3}{10}\,\zeta_3\right)\varepsilon^{-1}$
9	$e112\|23\|e4\|455\|55\|\|$	1/4	$r_1^2\, r_2^2$	$-\frac{7}{720}\,\varepsilon^{-4}+\frac{37}{720}\,\varepsilon^{-3}-\frac{307}{2880}\,\varepsilon^{-2}+\left(-\frac{1}{240}+\frac{1}{120}\,\zeta_3\right)\varepsilon^{-1}$
10	$e112\|33\|344\|5\|55\|e\|$	1/16	$r_1\, r_{14}$	$-\frac{7}{180}\,\varepsilon^{-5}+\frac{3}{40}\,\varepsilon^{-4}+\frac{7}{720}\,\varepsilon^{-3}+\left(-\frac{59}{480}+\frac{1}{10}\,\zeta_3\right)\varepsilon^{-2}+\left(\frac{959}{2880}+\frac{3}{20}\,\zeta_4-\frac{1}{20}\,\zeta_3\right)\varepsilon^{-1}$
11	$e112\|33\|444\|55\|5\|e\|$	1/48	$r_1^2\, r_4$	$-\frac{1}{40}\,\varepsilon^{-4}+\frac{13}{320}\,\varepsilon^{-3}+\frac{29}{320}\,\varepsilon^{-2}+\left(\frac{221}{1280}-\frac{7}{80}\,\zeta_3\right)\varepsilon^{-1}$
12	$e112\|33\|445\|45\|5\|e\|$	1/4	$r_1\, r_{13}$	$-\frac{13}{720}\,\varepsilon^{-5}+\frac{103}{1440}\,\varepsilon^{-4}-\frac{377}{2880}\,\varepsilon^{-3}+\left(\frac{155}{1152}-\frac{19}{120}\,\zeta_3\right)\varepsilon^{-2}+\left(\frac{703}{1280}-\frac{1}{20}\,\zeta_4-\frac{1}{48}\,\zeta_3\right)\varepsilon^{-1}$
13	$e112\|33\|445\|e5\|55\|\|$	1/16	$r_1^2\, r_2^2$	$-\frac{1}{72}\,\varepsilon^{-4}+\frac{1}{18}\,\varepsilon^{-3}-\frac{7}{288}\,\varepsilon^{-2}-\frac{11}{24}\,\varepsilon^{-1}$
14	$e112\|33\|e34\|5\|555\|\|$	1/12	$r_1^2\, r_4$	$-\frac{13}{720}\,\varepsilon^{-4}+\frac{197}{2880}\,\varepsilon^{-3}-\frac{1}{48}\,\varepsilon^{-2}+\left(-\frac{223}{2304}-\frac{1}{48}\,\zeta_3\right)\varepsilon^{-1}$
15	$e112\|33\|e44\|55\|55\|\|$	1/32	$r_1\, r_{15}$	$-\frac{1}{12}\,\varepsilon^{-5}+\frac{1}{24}\,\varepsilon^{-4}+\frac{5}{48}\,\varepsilon^{-3}+\left(\frac{13}{96}-\frac{1}{6}\,\zeta_3\right)\varepsilon^{-2}+\left(\frac{29}{192}-\frac{1}{4}\,\zeta_4+\frac{1}{12}\,\zeta_3\right)\varepsilon^{-1}$
16	$e112\|33\|e45\|45\|55\|\|$	1/8	$r_1\, r_9$	$-\frac{1}{36}\,\varepsilon^{-5}+\frac{31}{360}\,\varepsilon^{-4}-\frac{13}{240}\,\varepsilon^{-3}+\left(-\frac{11}{288}-\frac{1}{60}\,\zeta_3\right)\varepsilon^{-2}+\left(-\frac{511}{2880}-\frac{1}{40}\,\zeta_4+\frac{23}{120}\,\zeta_3\right)\varepsilon^{-1}$
17	$e112\|34\|334\|5\|55\|e\|$	1/8	$r_1\, r_{10}$	$-\frac{1}{72}\,\varepsilon^{-5}+\frac{13}{240}\,\varepsilon^{-4}-\frac{17}{288}\,\varepsilon^{-3}+\left(\frac{5}{192}-\frac{1}{10}\,\zeta_3\right)\varepsilon^{-2}+\left(-\frac{341}{5760}-\frac{3}{20}\,\zeta_4+\frac{7}{60}\,\zeta_3\right)\varepsilon^{-1}$
18	$e112\|34\|335\|4\|55\|e\|$	1/8	$r_1\, r_{12}$	$-\frac{1}{72}\,\varepsilon^{-5}+\frac{13}{240}\,\varepsilon^{-4}-\frac{17}{288}\,\varepsilon^{-3}+\left(\frac{5}{192}+\frac{1}{15}\,\zeta_3\right)\varepsilon^{-2}+\left(-\frac{341}{5760}-\frac{11}{40}\,\zeta_4+\frac{9}{20}\,\zeta_3\right)\varepsilon^{-1}$
19	$e112\|34\|335\|5\|e55\|\|$	1/4	$r_1\, r_{11}$	$-\frac{7}{360}\,\varepsilon^{-5}+\frac{1}{15}\,\varepsilon^{-4}-\frac{37}{720}\,\varepsilon^{-3}+\left(-\frac{17}{480}-\frac{1}{60}\,\zeta_3\right)\varepsilon^{-2}+\left(\frac{553}{2880}-\frac{1}{40}\,\zeta_4-\frac{19}{120}\,\zeta_3\right)\varepsilon^{-1}$
20	$e112\|34\|335\|e\|555\|\|$	1/24	$r_1^2\, r_3$	$-\frac{7}{480}\,\varepsilon^{-4}+\frac{11}{240}\,\varepsilon^{-3}+\frac{7}{384}\,\varepsilon^{-2}+\frac{3}{256}\,\varepsilon^{-1}$
21	$e112\|34\|345\|45\|5\|e\|$	1/2	$r_1\, r_2\, r_3$	$-\frac{4}{15}\,\zeta_3\,\varepsilon^{-3}+\left(\frac{1}{10}\,\zeta_4+\frac{19}{30}\,\zeta_3\right)\varepsilon^{-2}+\left(-\frac{17}{40}\,\zeta_4-\frac{13}{10}\,\zeta_3+\frac{21}{20}\,\zeta_5\right)\varepsilon^{-1}$
22	$e112\|34\|345\|e5\|55\|\|$	1/2	$r_1\, r_{10}$	$-\frac{1}{180}\,\varepsilon^{-5}+\frac{29}{720}\,\varepsilon^{-4}-\frac{217}{1440}\,\varepsilon^{-3}+\left(\frac{1019}{2880}-\frac{7}{30}\,\zeta_3\right)\varepsilon^{-2}+\left(-\frac{1903}{1920}+\frac{1}{40}\,\zeta_4+\frac{3}{5}\,\zeta_3\right)\varepsilon^{-1}$

Table A.2 (*continued*)

N	NI(γ)	s_γ	r_γ	$\partial_{p^2} K R' \gamma$
23	$e112\|34\|355\|45\|e5\|\|$	1/2	$r_1\, r_{10}$	$-\frac{1}{180}\,\varepsilon^{-5}+\frac{29}{720}\,\varepsilon^{-4}-\frac{217}{1440}\,\varepsilon^{-3}+\left(\frac{1019}{2880}-\frac{1}{15}\,\zeta_3\right)\varepsilon^{-2}+\left(-\frac{1903}{1920}-\frac{1}{10}\,\zeta_4+\frac{3}{5}\,\zeta_3\right)\varepsilon^{-1}$
24	$e112\|34\|355\|e4\|55\|\|$	1/4	$r_1\, r_{13}$	$-\frac{1}{90}\,\varepsilon^{-5}+\frac{1}{24}\,\varepsilon^{-4}-\frac{13}{720}\,\varepsilon^{-3}-\frac{11}{480}\,\varepsilon^{-2}+\left(-\frac{1769}{2880}+\frac{7}{20}\,\zeta_3\right)\varepsilon^{-1}$
25	$e112\|34\|e33\|5\|555\|\|$	1/24	$r_1^2\, r_4$	$-\frac{13}{720}\,\varepsilon^{-4}+\frac{197}{2880}\,\varepsilon^{-3}-\frac{1}{48}\,\varepsilon^{-2}+\left(-\frac{223}{2304}-\frac{1}{48}\,\zeta_3\right)\varepsilon^{-1}$
26	$e112\|34\|e34\|55\|55\|\|$	1/8	$r_1\, r_{14}$	$-\frac{1}{72}\,\varepsilon^{-5}+\frac{11}{240}\,\varepsilon^{-4}+\frac{53}{1440}\,\varepsilon^{-3}+\left(-\frac{61}{192}+\frac{17}{60}\,\zeta_3\right)\varepsilon^{-2}+\left(\frac{157}{5760}+\frac{1}{20}\,\zeta_4-\frac{7}{40}\,\zeta_3\right)\varepsilon^{-1}$
27	$e112\|34\|e35\|45\|55\|\|$	1/2	$r_1\, r_{13}$	$-\frac{1}{144}\,\varepsilon^{-5}+\frac{71}{1440}\,\varepsilon^{-4}-\frac{101}{576}\,\varepsilon^{-3}+\left(\frac{1319}{5760}-\frac{11}{120}\,\zeta_3\right)\varepsilon^{-2}+\left(\frac{29}{3840}+\frac{1}{20}\,\zeta_4+\frac{11}{240}\,\zeta_3\right)\varepsilon^{-1}$
28	$e112\|34\|e55\|445\|5\|\|$	1/16	$r_1\, r_9$	$-\frac{1}{36}\,\varepsilon^{-5}+\frac{31}{360}\,\varepsilon^{-4}-\frac{13}{240}\,\varepsilon^{-3}+\left(-\frac{11}{288}-\frac{1}{60}\,\zeta_3\right)\varepsilon^{-2}+\left(-\frac{511}{2880}-\frac{1}{40}\,\zeta_4+\frac{23}{120}\,\zeta_3\right)\varepsilon^{-1}$
29	$e112\|e3\|334\|5\|555\|\|$	1/24	r_1^3	$-\frac{1}{384}\,\varepsilon^{-3}+\frac{5}{128}\,\varepsilon^{-2}-\frac{7}{32}\,\varepsilon^{-1}$
30	$e112\|e3\|344\|55\|55\|\|$	1/16	$r_1^2\, r_4$	$-\frac{1}{160}\,\varepsilon^{-4}+\frac{3}{80}\,\varepsilon^{-3}-\frac{53}{640}\,\varepsilon^{-2}+\left(\frac{59}{1280}+\frac{7}{80}\,\zeta_3\right)\varepsilon^{-1}$
31	$e112\|e3\|345\|45\|55\|\|$	1/8	$r_1^2\, r_3$	$-\frac{1}{480}\,\varepsilon^{-4}+\frac{11}{480}\,\varepsilon^{-3}-\frac{71}{640}\,\varepsilon^{-2}+\left(\frac{293}{1280}+\frac{7}{40}\,\zeta_3\right)\varepsilon^{-1}$
32	$e112\|e3\|444\|555\|5\|\|$	1/72	r_1^3	$-\frac{1}{192}\,\varepsilon^{-3}+\frac{5}{192}\,\varepsilon^{-2}-\frac{11}{384}\,\varepsilon^{-1}$
33	$e112\|e3\|445\|455\|5\|\|$	1/8	$r_1^2\, r_3$	$-\frac{1}{240}\,\varepsilon^{-4}+\frac{17}{480}\,\varepsilon^{-3}-\frac{173}{960}\,\varepsilon^{-2}+\left(\frac{1249}{1920}-\frac{3}{20}\,\zeta_3\right)\varepsilon^{-1}$
34	$e123\|224\|4\|555\|e5\|\|$	1/24	$r_1^2\, r_3$	$-\frac{1}{120}\,\varepsilon^{-4}+\frac{11}{320}\,\varepsilon^{-3}-\frac{3}{80}\,\varepsilon^{-2}+\left(\frac{401}{3840}-\frac{7}{40}\,\zeta_3\right)\varepsilon^{-1}$
35	$e123\|224\|5\|445\|5\|e\|$	1/4	$r_1\, r_{10}$	$-\frac{1}{120}\,\varepsilon^{-5}+\frac{11}{240}\,\varepsilon^{-4}-\frac{49}{480}\,\varepsilon^{-3}+\left(\frac{47}{960}-\frac{1}{10}\,\zeta_3\right)\varepsilon^{-2}+\left(\frac{261}{640}-\frac{3}{20}\,\zeta_4+\frac{7}{60}\,\zeta_3\right)\varepsilon^{-1}$
36	$e123\|234\|45\|45\|5\|e\|$	1/2	$r_1\, r_8$	$\frac{5}{3}\,\zeta_5\,\varepsilon^{-2}+\left(-\frac{25}{12}\,\zeta_6+\frac{1}{6}\,\zeta_3^2\right)\varepsilon^{-1}$
37	$e123\|234\|45\|55\|e5\|\|$	1/2	$r_1\, r_2\, r_3$	$-\frac{1}{10}\,\zeta_3\,\varepsilon^{-3}+\left(-\frac{3}{20}\,\zeta_4+\frac{11}{20}\,\zeta_3\right)\varepsilon^{-2}+\left(-\frac{3}{10}\,\zeta_4-\frac{7}{40}\,\zeta_3-\frac{1}{30}\,\zeta_5\right)\varepsilon^{-1}$
38	$e123\|245\|45\|445\|\|e\|$	1/4	$r_1\, r_2\, r_3$	$-\frac{1}{10}\,\zeta_3\,\varepsilon^{-3}+\left(-\frac{3}{20}\,\zeta_4+\frac{11}{20}\,\zeta_3\right)\varepsilon^{-2}+\left(-\frac{3}{10}\,\zeta_4-\frac{7}{40}\,\zeta_3+\frac{23}{60}\,\zeta_5\right)\varepsilon^{-1}$
39	$e123\|e23\|34\|5\|555\|\|$	1/12	$r_1^2\, r_3$	$-\frac{1}{288}\,\varepsilon^{-4}+\frac{25}{576}\,\varepsilon^{-3}-\frac{91}{384}\,\varepsilon^{-2}+\left(\frac{583}{1152}+\frac{1}{24}\,\zeta_3\right)\varepsilon^{-1}$
40	$e123\|e23\|44\|55\|55\|\|$	1/16	$r_1\, r_9$	$-\frac{1}{120}\,\varepsilon^{-5}+\frac{7}{240}\,\varepsilon^{-4}+\frac{11}{480}\,\varepsilon^{-3}+\left(-\frac{197}{960}+\frac{2}{15}\,\zeta_3\right)\varepsilon^{-2}+\left(\frac{443}{1920}+\frac{23}{40}\,\zeta_4-\frac{43}{60}\,\zeta_3\right)\varepsilon^{-1}$
41	$e123\|e23\|45\|45\|55\|\|$	1/8	$r_1\, r_{11}$	$-\frac{1}{360}\,\varepsilon^{-5}+\frac{17}{720}\,\varepsilon^{-4}-\frac{11}{160}\,\varepsilon^{-3}+\left(-\frac{587}{2880}+\frac{13}{30}\,\zeta_3\right)\varepsilon^{-2}+\left(\frac{10\,453}{5760}-\frac{1}{10}\,\zeta_4-\frac{101}{60}\,\zeta_3\right)\varepsilon^{-1}$
42	$e123\|e24\|33\|5\|555\|\|$	1/6	$r_1^2\, r_3$	$-\frac{7}{960}\,\varepsilon^{-4}+\frac{1}{30}\,\varepsilon^{-3}-\frac{11}{768}\,\varepsilon^{-2}+\left(-\frac{73}{512}+\frac{1}{24}\,\zeta_3\right)\varepsilon^{-1}$
43	$e123\|e24\|34\|55\|55\|\|$	1/4	$r_1\, r_{13}$	$-\frac{1}{360}\,\varepsilon^{-5}+\frac{1}{48}\,\varepsilon^{-4}-\frac{77}{1440}\,\varepsilon^{-3}+\left(-\frac{31}{960}+\frac{2}{15}\,\zeta_3\right)\varepsilon^{-2}+\left(\frac{2243}{5760}-\frac{7}{40}\,\zeta_4-\frac{1}{4}\,\zeta_3\right)\varepsilon^{-1}$
44	$e123\|e24\|35\|45\|55\|\|$	1	$r_1\, r_{10}$	$-\frac{1}{720}\,\varepsilon^{-5}+\frac{5}{288}\,\varepsilon^{-4}-\frac{347}{2880}\,\varepsilon^{-3}+\left(\frac{3037}{5760}-\frac{11}{60}\,\zeta_3\right)\varepsilon^{-2}+\left(-\frac{1323}{1280}+\frac{1}{10}\,\zeta_4+\frac{13}{24}\,\zeta_3\right)\varepsilon^{-1}$
45	$e123\|e24\|55\|445\|5\|\|$	1/4	$r_1\, r_{11}$	$-\frac{1}{240}\,\varepsilon^{-5}+\frac{13}{480}\,\varepsilon^{-4}-\frac{11}{192}\,\varepsilon^{-3}+\left(-\frac{239}{1920}+\frac{1}{12}\,\zeta_3\right)\varepsilon^{-2}+\left(\frac{1211}{1280}+\frac{1}{8}\,\zeta_4-\frac{97}{120}\,\zeta_3\right)\varepsilon^{-1}$

(*continued on next page*)

Table A.2 (*continued*)

N	NI(γ)	s_γ	r_γ	$\partial_{p^2} K R' \gamma$
46	$e123\|e45\|334\|5\|55\|\|$	1/8	$r_1\, r_{11}$	$-\frac{1}{90}\,\varepsilon^{-5} + \frac{1}{20}\,\varepsilon^{-4} - \frac{17}{360}\,\varepsilon^{-3} + \left(-\frac{19}{240} + \frac{1}{60}\,\zeta_3\right)\varepsilon^{-2} + \left(-\frac{49}{1440} + \frac{1}{40}\,\zeta_4 - \frac{3}{40}\,\zeta_3\right)\varepsilon^{-1}$
47	$e123\|e45\|344\|55\|5\|\|$	1/8	$r_1\, r_{12}$	$-\frac{1}{360}\,\varepsilon^{-5} + \frac{1}{48}\,\varepsilon^{-4} - \frac{77}{1440}\,\varepsilon^{-3} + \left(-\frac{31}{960} + \frac{2}{15}\,\zeta_3\right)\varepsilon^{-2} + \left(\frac{2243}{5760} - \frac{7}{40}\,\zeta_4 - \frac{1}{4}\,\zeta_3\right)\varepsilon^{-1}$
48	$e123\|e45\|345\|45\|5\|\|$	1/4	$r_1\, r_2\, r_3$	$-\frac{1}{6}\,\zeta_3\,\varepsilon^{-3} + \left(\frac{1}{4}\,\zeta_4 + \frac{7}{12}\,\zeta_3\right)\varepsilon^{-2} + \left(-\frac{1}{2}\,\zeta_4 - \frac{5}{8}\,\zeta_3 + \frac{2}{3}\,\zeta_5\right)\varepsilon^{-1}$
49	$e123\|e45\|444\|555\|\|\|$	1/72	r_1^3	$-\frac{1}{192}\,\varepsilon^{-3} + \frac{5}{192}\,\varepsilon^{-2} - \frac{11}{384}\,\varepsilon^{-1}$
50	$e123\|e45\|445\|455\|\|\|$	1/8	$r_1\, r_{10}$	$-\frac{1}{360}\,\varepsilon^{-5} + \frac{1}{48}\,\varepsilon^{-4} - \frac{77}{1440}\,\varepsilon^{-3} + \left(-\frac{31}{960} - \frac{1}{30}\,\zeta_3\right)\varepsilon^{-2} + \left(\frac{2243}{5760} - \frac{1}{20}\,\zeta_4 - \frac{1}{4}\,\zeta_3\right)\varepsilon^{-1}$

Table A.3
Values of the factors $r_i(n)$ in A.2.

i	$r_i(n)$	i	$r_i(n)$
1	$(n+2)/3$	9	$(3n^3+24n^2+80n+136)/243$
2	$(n+8)/9$	10	$(7n^2+72n+164)/243$
3	$(5n+22)/27$	11	$(11n^2+76n+156)/243$
4	$(n^2+6n+20)/27$	12	$(n^3+10n^2+72n+160)/243$
5	$(3n^2+22n+56)/81$	13	$(n^3+14n^2+76n+152)/243$
6	$(n^2+20n+60)/81$	14	$(n^3+18n^2+80n+144)/243$
7	$(n^3+8n^2+24n+48)/81$	15	$(n^4+10n^3+40n^2+80n+112)/243$
8	$(2n^2+55n+186)/243$		

Appendix B. Extended 't Hooft condition for separate diagrams

In this Appendix we discuss an extension[5] of the well-known 't Hooft constraints originally suggested in [9] for global renormalization constants (that is, ones including all contributions up to some number of loops) to a case when one deals with a separate Feynman integral.

Let Γ be a particular L-loop OPI Feynman diagram without any IR (sub)divergences.[6] Without essential loss of generality we assume that $\langle\Gamma\rangle(Q^2, \mu^2)$ is a scalar integral depending on the external momentum Q via its square, $Q^2 = Q_\nu Q^\nu$. In addition, we introduce the renormalization scale parameter μ into the definition of every bare dimensionally regulated FI by providing it with a factor $(\mu^2)^{L\,\varepsilon}$.

The renormalized version of the corresponding Feynman integral can be generically written as

$$R\,\langle\Gamma\rangle(Q^2, \mu^2) = \langle\Gamma\rangle(Q^2, \mu^2) + Z_\Gamma + \boxed{\sum_\gamma Z_\gamma \langle\Gamma/\gamma\rangle(Q^2) + \ldots} \tag{B.1}$$

Here Z_γ is the UV Z-factor corresponding to a OPI subgraph γ of Γ, Z_Γ is the UV counterterm for the very FI $\langle\Gamma\rangle$ and dots stand for contributions with two and more UV subtractions.

[5] We do not claim that the extension is an original contribution of us. In fact, at least for IR-finite diagrams it is well-known among experts since long. For instance, very recently similar considerations have been effectively employed in [46] to study divergences in maximal supersymmetric Yang–Mills theories in diverse dimensions.

[6] This constraint will be relaxed later.

Every particular term in the boxed part of eq. (B.1) is a product of some Z-factors and a reduced FI, the latter by construction includes a factor $(\mu^2)^{n\varepsilon}$, with n being its loop number.

The finiteness of the left part of eq. (B.1) together with the fact that the Z_γ has no dependence on μ leads to a number of interesting consequences. For instance, if $L = 2$ then only the knowledge of the pole parts of the *one-loop* subgraphs of Γ as well as one-loop reduced FI $\langle\Gamma/\gamma\rangle$ allows one to construct the leading $1/\varepsilon^2$ poles of the FI $\langle\Gamma\rangle$ and the counterterm Z_Γ. By induction, one could easily infer that for arbitrary number of loops L the leading $1/\varepsilon^L$ poles of both the FI $\langle\Gamma\rangle$ and the corresponding counterterm Z_Γ can be completely restored from the pole parts (read UV counterterms) of properly constructed set of one-loop FIs. The set includes all graphs of the form γ/γ', with γ and γ' being two OPI subgraphs of Γ such that $\gamma' \subset \gamma$ and $L_\gamma - L_{\gamma'} = 1$.

In the same way one could infer *subleading* poles of order $1/\varepsilon^{L-1}$ exclusively from knowledge of Z-factors from similarly constructed set of two-loop FIs. And so on and forth. This is, obviously, the diagram-wise formulation of the 't Hoof constraints.

Another simple (but still useful) observation is that the knowledge of Z_Γ and all the boxed terms in the r.h.s. of (B.1) is enough to *completely* restore the pole part of the original bare FI $\langle\Gamma\rangle$.

In fact, all the above considerations are easily generalized for a case when FI $\langle\Gamma\rangle$ is suffering from IR divergences in addition to UV ones.[7] Indeed, as it should be clear from the general discussion of section 3 it suffices to employ the R^*-operation instead of the usual R-one.

Finally, let us now assume that the FI $\langle\Gamma\rangle$ is a massless five-loop propagator-like FI. Combining two facts: (i) 5-loop Z-factors are all computable in terms of 4-loop p-integrals and (ii) every reduced FI in the r.h.s. of (B.1) is a p-integral with its loop number not exceeding 4, we arrive at a conclusion that the pole part of $\langle\Gamma\rangle$ is expressible in terms of 4-loop p-integrals.

As an example we present here complete expression for pole part of the five loop p-integral from section 5.1:

$$K\left(\quad\right). \tag{B.2}$$

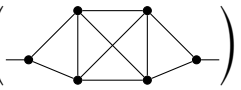

Taking into account that

$$K\,R'\left(\quad\right) = K\,R^{*\prime}\left(\quad\right), \tag{B.3}$$

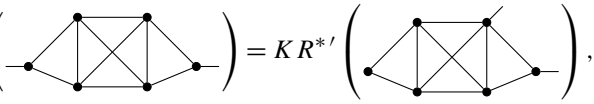

and r.h.s. is computable in terms of 4-loop p-integrals, and expanding R' operation in the l.h.s. of the (B.3) we arrive at the following relation:

$$K\left(\quad\right)$$

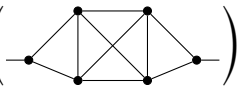

$$= K\left(R^{*\prime}\left(\quad\right) + K\,R'\left(\quad\right)\quad\right) +$$

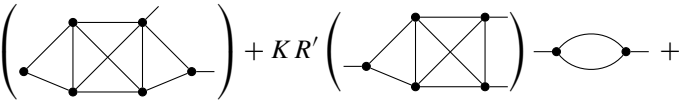

[7] This statement is only valid for Euclidean case, as the very R^*-operation is not suitable to deal with more complicated (collinear, etc.) IR singularities which might appear in Minkowskian FIs.

$$+ K R' \left(\right) \quad + K R' \left(\right) \quad . \tag{B.4}$$

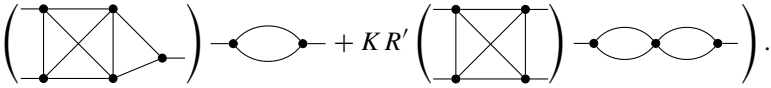

Here all terms of r.h.s. of (B.4) can be expressed in terms of 4-loop p-integrals.

Appendix C. $1/n$-expansion

In paper [37] conformal bootstrap technique was applied to calculate $1/n$-expansion of the critical exponent η up to $1/n^3$ term:

$$\eta = \frac{\eta_1}{n} + \frac{\eta_2}{n^2} + \frac{\eta_3}{n^3} + \mathcal{O}\left(\frac{1}{n^4}\right). \tag{C.1}$$

It is possible to compare results obtained using ε-expansion with results of $1/n$-expansion for this exponent: while ε-expansion is an exact function of n, $1/n$-expansion calculated in [37] is an exact function of ε. Thus twofold series of both expansions must coincide.

Unfortunately, η_3 in [37] contain misprint, so we present corrected version here:

$$\eta_1 = -\frac{4\Gamma(d-2)}{\Gamma(2-d/2)\Gamma(d/2-2)\Gamma(d/2-1)\Gamma(d/2+1)}, \tag{C.2}$$

$$\frac{\eta_2}{\eta_1^2} = \frac{d^2-3d+4}{4-d} R_0 + \frac{1}{d} + \frac{1}{d-2} + \frac{9}{4-d} + \frac{4}{(4-d)^2} - 2 - d, \tag{C.3}$$

where $R_0 = \psi(d-2) + \psi(2-d/2) - \psi(2) - \psi(d/2-2)$ and $\psi(x) = \frac{d}{dx} \ln \Gamma(x)$. Furthermore,

$$\begin{aligned}
\frac{\eta_3}{\eta_1^3} = {} & \frac{3d^2(d-2)(2d-5) I(d/2) S_3}{4(4-d)^2} + \frac{2}{3} \frac{d^2(d-2)(d-3)^2(3S_0S_1 - S_0^3 - S_2)}{(4-d)^3} + \\
& + 35 + \frac{13}{2}d + d^2 - \frac{177}{4-d} + \frac{134}{(4-d)^2} + \frac{232}{(4-d)^2} - \frac{128}{(4-d)^3} + \frac{9}{d-2} + \frac{2}{(d-2)^2} + \\
& + \frac{2}{d^2} + \frac{B}{2}\left(66 + 7d + d^2 - \frac{374}{4-d} + \frac{408}{(4-d)^2} + \frac{128}{(4-d)^3} + \frac{4}{d-2} + \frac{6}{d}\right) + \\
& + \frac{B^2}{2}\left(20 - \frac{100}{4-d} + \frac{128}{(4-d)^2}\right) + \\
& + \frac{S_3}{2}\left(-45 - 5d + \frac{7}{4}d^2 + \frac{254}{4-d} - \frac{256}{(4-d)^2} - \frac{384}{(4-d)^3} + \frac{512}{(4-d)^4}\right) + \\
& + \frac{S_4}{2}\left(14 + 4d + 2d^2 - \frac{60}{4-d}\right) + \\
& + \frac{BS_3}{2}\left(-45 - \frac{13}{2}d - \frac{1}{2}d^2 + \frac{272}{4-d} - \frac{432}{(4-d)^2} + \frac{256}{(4-d)^3}\right),
\end{aligned} \tag{C.4}$$

where

$$\begin{aligned}
B &= \psi(2-d/2) + \psi(d-2) - 1 + \gamma_E - \psi(d/2-2), \\
S_0 &= \psi(2-d/2) + \psi(d-2) + \gamma_E - \psi(d/2-1), \\
S_1 &= \psi'(2-d/2) - \psi'(d-2) - \zeta(2) + \psi'(d/2-1), \\
S_2 &= \psi''(2-d/2) + \psi''(d-2) + 2\zeta(3) - \psi''(d/2-1),
\end{aligned}$$

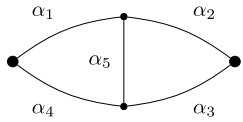

Fig. C.6. T-bubble graph contributing to η_3 ($\alpha_1 = \alpha_4 = 1$, $\alpha_2 = \alpha_3 = d/2 - 1$, $\alpha_5 = d/2 - 1 + \Delta$).

$$S_3 = \psi'(d/2 - 1) - \psi'(1),$$
$$S_4 = \psi''(2 - d/2) - \psi'(d - 2), \tag{C.5}$$

γ_E is Euler constant and value $I(d)$ is determined from the relation:

$$\Pi(d, \Delta) = \Pi(d, 0)\left(1 + I(d)\,\Delta + \mathcal{O}(\Delta^2)\right). \tag{C.6}$$

Here $\Pi(d, \Delta)$ is value of the diagram on Fig. C.6 (in x-space) with $\alpha_1 = \alpha_4 = 1$, $\alpha_2 = \alpha_3 = d/2 - 1$, $\alpha_5 = d/2 - 1 + \Delta$.

Given the value of the $I(d)$ for any d one can construct $1/n$ expansion for arbitrary space dimension. The value of $I(4 - 2\varepsilon)$ can be extracted from [47] with the result:

$$I(4 - 2\varepsilon) = -\frac{5\zeta(5)}{2\zeta(3)}\varepsilon + \left(\frac{15\zeta(4)\zeta(5) - 25\zeta(3)\zeta(6) + 10\zeta(3)^3}{4\zeta(3)^2}\right)\varepsilon^2 + \mathcal{O}(\varepsilon^3). \tag{C.7}$$

Combining (C.1)–(C.5) with (C.7) and expanding it in ε up to ε^6 term, and, from another hand, expanding (20) in $1/n$ up to $1/n^3$ term we arrive at two *identical* expansions with

$$\eta_1 = 2\,\varepsilon^2 - \varepsilon^3 - \frac{5}{2}\,\varepsilon^4 + \left(-\frac{13}{4} + 4\,\zeta_3\right)\varepsilon^5 + \left(-\frac{29}{8} - 2\,\zeta_3 + 6\,\zeta_4\right)\varepsilon^6 + \mathcal{O}(\varepsilon^7)$$
$$\eta_2 = -28\,\varepsilon^2 + 86\,\varepsilon^3 + (-35 - 176\,\zeta_3)\,\varepsilon^5 + \left(-\frac{243}{4} + 488\,\zeta_3 - 264\,\zeta_4\right)\varepsilon^6 + \mathcal{O}(\varepsilon^7)$$
$$\eta_3 = 320\,\varepsilon^2 - 1984\,\varepsilon^3 + (2732 - 960\,\zeta_3)\,\varepsilon^4 +$$
$$+ (686 + 9440\,\zeta_3 - 1440\,\zeta_4 + 2560\,\zeta_5)\,\varepsilon^5 +$$
$$+ \left(799 - 28\,104\,\zeta_3 + 14\,160\,\zeta_4 + 1024\,\zeta_3^2 + 6400\,\zeta_6 - 24\,400\,\zeta_5\right)\varepsilon^6 + \mathcal{O}(\varepsilon^7). \tag{C.8}$$

Two comments are required here. First, equality of the twofold series produces three independent relations for six loop diagram values (only one six loop diagram contributes to $1/n$ term, to $1/n^2$ contributes 20 diagrams, and to $1/n^3$ – 50 diagrams, i.e. all six loop diagrams). So comparison with the $1/n$ expansion should be considered as a really strong check of our six loop results. Second, actually only the first term from $I(d)$ (of order ε) is required for six loops, the next term of $I(d)$ will contribute to seven loop term, but to get the same kind of relations (which touch all seven loop diagrams) one would need to calculate $1/n^4$ contribution to (C.1).

Appendix D. Supplementary material

Supplementary material related to this article can be found online at http://dx.doi.org/10.1016/j.nuclphysb.2016.03.009.

References

[1] K.G. Wilson, Phys. Rev. Lett. 28 (1972) 548.
[2] E. Brezin, J.C. Le Guillou, J. Zinn-Justin, B.G. Nickel, Phys. Lett. A 44 (1973) 227.
[3] A.A. Vladimirov, D.I. Kazakov, O.V. Tarasov, Sov. Phys. JETP 50 (1979) 521.
[4] K.G. Chetyrkin, A.L. Kataev, F.V. Tkachev, Phys. Lett. B 99 (1981) 147;
K.G. Chetyrkin, A.L. Kataev, F.V. Tkachev, Phys. Lett. B 101 (1981) 457 (Erratum).
[5] K.G. Chetyrkin, S.G. Gorishny, S.A. Larin, F.V. Tkachov, Phys. Lett. B 132 (1983) 351;
K.G. Chetyrkin, S.G. Gorishny, S.A. Larin, F.V. Tkachov, preprint INR P-0453, Moscow, 1986.
[6] D.I. Kazakov, Phys. Lett. B 133 (1983) 406;
D.I. Kazakov, Theor. Math. Phys. 58 (1984) 223–230;
D.I. Kazakov, Teor. Mat. Fiz. 58 (1984) 343–353.
[7] H. Kleinert, J. Neu, V. Shulte-Frohlinde, K.G. Chetyrkin, S.A. Larin, Phys. Lett. B 272 (1991) 39;
H. Kleinert, J. Neu, V. Shulte-Frohlinde, K.G. Chetyrkin, S.A. Larin, Phys. Lett. B 319 (1993) 545 (Erratum).
[8] L.Ts. Adzhemyan, M.V. Kompaniets, J. Phys. Conf. Ser. 523 (2014) 012049.
[9] G. 't Hooft, Dimensional regularization and the renormalization group, Nucl. Phys. B 61 (1973) 455–468.
[10] J.C. Collins, Normal products in dimensional regularization, Nucl. Phys. B 92 (1975) 477.
[11] N.N. Bogoliubov, O.S. Parasiuk, Acta Math. 97 (1957) 227.
[12] N.N. Bogoliubov, D.V. Shirkov, Introduction to the Theory of Quantized Fields, Nauka, Moscow, 1976 (in Russian); English transl.: Interscience, New York, 1980.
[13] A.A. Vladimirov, Theor. Math. Phys. 43 (1980) 417.
[14] K.G. Chetyrkin, A.L. Kataev, F.V. Tkachov, Nucl. Phys. B 174 (1980) 345.
[15] O.V. Tarasov, A.A. Vladimirov, Sov. J. Nucl. Phys. 25 (1977) 585.
[16] D.I. Kazakov, O.V. Tarasov, A.A. Vladimirov, Sov. Phys. JETP 50 (1979) 521.
[17] O.V. Tarasov, A.A. Vladimirov, A.Y. Zharkov, Phys. Lett. B 93 (1980) 429.
[18] K.G. Chetyrkin, V.A. Smirnov, Phys. Lett. B 144 (1984) 419.
[19] K.G. Chetyrkin, Phys. Lett. B 390 (1997) 309, arXiv:hep-ph/9608318.
[20] K.G. Chetyrkin, Phys. Lett. B 391 (1997) 402, arXiv:hep-ph/9608480.
[21] M. Misiak, M. Münz, Phys. Lett. B 344 (1995) 308, arXiv:hep-ph/9409454.
[22] K.G. Chetyrkin, M. Misiak, M. Münz, Phys. Lett. B 400 (1997) 206, arXiv:hep-ph/9612313.
[23] T. van Ritbergen, J.A.M. Vermaseren, S.A. Larin, Phys. Lett. B 400 (1997) 379, arXiv:hep-ph/9701390.
[24] W.E. Caswell, A.D. Kennedy, Phys. Rev. D 25 (1982) 392.
[25] P.A. Baikov, K.G. Chetyrkin, J.H. Kuhn, J. Rittinger, J. High Energy Phys. 1207 (2012) 017, arXiv:1206.1284 [hep-ph].
[26] B. Eden, P. Heslop, G.P. Korchemsky, V.A. Smirnov, E. Sokatchev, Nucl. Phys. B 862 (2012) 123, arXiv:1202.5733 [hep-th].
[27] K.G. Chetyrkin, Combinatorics of R, R^{-1} and R^* operations and asymptotic expansions of Feynman integrals in the limit of large momenta and masses, preprint MPI-Ph/PTh13/91, 1991.
[28] D. Batkovich, M. Kompaniets, Toolbox for multiloop Feynman diagrams calculations using R^* operation, J. Phys. Conf. Ser. 608 (1) (2015) 012068, arXiv:1411.2618 [hep-th].
[29] P.A. Baikov, K.G. Chetyrkin, J.H. Kühn, Nucl. Part. Phys. Proc. 261–262 (2015) 3, arXiv:1501.06739 [hep-ph].
[30] J.A. Gracey, Phys. Rev. D 92 (2) (2015) 025012, arXiv:1506.03357 [hep-th].
[31] P.A. Baikov, K.G. Chetyrkin, Nucl. Phys. B 837 (2010) 186.
[32] R.N. Lee, A.V. Smirnov, V.A. Smirnov, Nucl. Phys. B 856 (2012) 95, arXiv:1108.0732 [hep-th].
[33] E. Panzer, Nucl. Phys. B 874 (2013) 567, arXiv:1305.2161 [hep-th].
[34] R.N. Lee, Presenting LiteRed: a tool for the loop integrals reduction, preprint, arXiv:1212.2685 [hep-ph], 2012;
R.N. Lee, J. Phys. Conf. Ser. 523 (2014) 012059, preprint, arXiv:1310.1145 [hep-ph].
[35] K.G. Chetyrkin, F.V. Tkachov, Nucl. Phys. B 192 (1981) 159.
[36] A.N. Vasiliev, Quantum Field Renormalization Group in Critical Behavior Theory and Stochastic Dynamics, Petersburg Inst. Nucl. Phys., St. Petersburg, 1998 (in Russian); English transl.: The Field Theoretic Renormalization Group in Critical Behavior Theory and Stochastic Dynamics, Chapman & Hall/CRC, Boca Raton, 2004.
[37] A.N. Vasil'ev, Yu.M. Pis'mak, Yu.R. Khonkonen, Teor. Mat. Fiz. 50 (2) (1982) 195–206;
A.N. Vasil'ev, Yu.M. Pis'mak, Yu.R. Khonkonen, Theor. Math. Phys. 50 (2) (1982) 127–134; this paper contains missprint in the second term of the r.h.s. of eq. (22): the denominator must be $3(2-\mu)^3$ (for details see [36] and Appendix C).
[38] T. Binoth, G. Heinrich, Nucl. Phys. B 585 (2000) 741–759, preprint, arXiv:hep-ph/0004013.

[39] D.I. Kazakov, D.V. Shirkov, Fortschr. Phys. 28 (1980) 465.
[40] D.I. Kazakov, D.V. Shirkov, O.V. Tarasov, Theor. Math. Phys. 38 (1979) 9;
D.I. Kazakov, D.V. Shirkov, O.V. Tarasov, Teor. Mat. Fiz. 38 (1979) 15.
[41] L.N. Lipatov, J. Exp. Theor. Phys. 72 (1977) 411.
[42] A. Pelissetto, E. Vicari, Phys. Rep. 368 (2002) 549–727, arXiv:cond-mat/0012164.
[43] D. Batkovich, M. Kompaniets, E. Panzer, in preparation.
[44] B. Nickel, D. Meiron, G. Baker, preprint, University of Guelf Report, 1977, http://users.physik.fu-berlin.de/~kleinert/nickel/guelph.pdf.
[45] D. Batkovich, Y. Kirienko, M. Kompaniets, S. Novikov, Graphstate – a tool for graph identification and labelling, preprint, arXiv:1409.8227 [hep-ph], 2014.
[46] L.V. Bork, D.I. Kazakov, M.V. Kompaniets, D.M. Tolkachev, D.E. Vlasenko, J. High Energy Phys. 1511 (2015) 059, arXiv:1508.05570 [hep-th].
[47] D.I. Kazakov, Teor. Mat. Fiz. 62 (1) (1985) 127–135;
D.I. Kazakov, Theor. Math. Phys. 62 (1) (1985) 84–89.